Desalination and Water Treatment
www.deswater.com

doi: 10.1080/19443994.2015.1085442

57 (2016) 17333–17342
August

Taylor & Francis
Taylor & Francis Group

Synthesis, characterization and performance evaluation of PVDF-SPES-ZrO_2 membrane

S.B. Mishra[a,*], Sadhana Sachan[a], S.N. Upadhyay[b], P.K. Mishra[b]

[a]*Department of Chemical Engineering, Motilal Nehru National Institute of Technology Allahabad, Allahabad 211 004, India, Tel. +91 532 227 1522; Fax: +91 532 2545341; emails: mishrass9753@gmail.com (S.B. Mishra), sadhanas@mnnit.ac.in (S. Sachan)*
[b]*Department of Chemical Engineering & Technology, Indian Institute of Technology (BHU), Varanasi 221005, India, emails: snupadhyay.che@itbhu.ac.in (S.N. Upadhyay), pkmishra.che@itbhu.ac.in (P.K. Mishra)*

Received 5 November 2014; Accepted 15 August 2015

ABSTRACT

Ultrafiltration (UF) membranes were prepared by blending different proportion of polyvinylidene fluoride (PVDF), sulphonated polyethersulphone (SPES) and nanoparticles of zirconium oxide (ZrO_2). The functional groups, surface and cross-sectional morphologies were analysed using Fourier transform infrared, scanning electron microscopy (SEM) and X-ray diffraction, respectively. The presence of particles and pores in the membrane is clearly revealed from the SEM photomicrographs. The effect of different transmembrane pressures is studied to evaluate the performance of membranes. The best value of the permeate flux with a low fouling recovery ratio is obtained at a transmembrane pressure of 0.3 MPa (3 bars). The performance of the membranes having 4 wt% ZrO_2 nanoparticles was studied with and without backwash. The backwashing is capable of restoring the initial flux to about 90%. SPES and ZrO_2 particles were found to play the role of antifouling agent and the hydrophilicity enhancer in the prepared composite membrane.

Keywords: Performance evaluation; UF membrane; Hydrophilic; Effluent treatment

1. Introduction

Incorporation of inorganic nanoparticles in polymeric membranes to improve membrane characteristics has received the attention of researchers in recent years. These membranes are usually prepared by blending solutions of two different polymers followed by the addition of nanoparticles of inorganic material. Polymeric membranes have the characteristic of smaller pore size, high porosity, high surface roughness, better chemical stability and better mechanical strength [1]. The membrane-based separation process is extensively used in wastewater treatment, especially in oil–water separation [2–12]. Most of these polymeric membranes have limited mechanical stability and efforts have been made to increase it by blending with different inorganic materials [13,14].

The process conditions, such as transmembrane pressure and feed concentration, play an important role in the membrane separation processes [15–19]. The membrane material should be thermally stable and chemically resistant. The polymers are still the main materials for membrane synthesis as they have good membrane-forming ability, wide variety, easy to

*Corresponding author.

module and are of low cost [2]. The fouling time, hydrophilicity and porous structure are other important characteristics of ultrafiltration (UF) membranes which control their application. In order to improve the hydrophilicity and strength and impart antifouling property, blending of appropriate organic and inorganic materials has been found to be a better option for membrane formation [14,15].

Among the various polymeric materials, polyvinylidene fluoride (PVDF) is widely used for membrane synthesis using phase inversion method. This polymer is thermally stable and can form asymmetric membranes which are good for UF process [2–6]. Since PVDF is hydrophobic in nature, blending of sulphonated polyethersulphone with it results in improvement of its fouling resistance, hydrophilicity and performance [15,19]. Addition of hydrophilic materials to the casting solution increases the water permeability of a membrane and thereby permeates flux [2,4]. The blends of organic polymer with various inorganic materials like alumina, titania, silica, zirconia and metal ions have also been investigated [19–21]. In our previous study, the purification of oily wastewater was reported using SPPEES–TiO_2 and PPEES–TiO_2 membranes [22,23].

Since, little published information is available on the impact of membrane characteristics on fouling improvement and solute rejection in a specific separation process [24–26]. Recently, a facile and effective technique to improve hydrophobic PVDF membrane using self-polymerize polydopamine and subsequent hydrolysis of ammonium fluotitanate were reported by Shao et al. [27]. In the recent development of water treatment, the application of mussel-inspired tailoring of membrane with wettability on the surface of membranes is investigated [28]. In this investigation, the flat sheets of hydrophilic composite membranes were prepared by phase inversion method using the blend of SPES–PVDF–ZrO_2. SPES and PVDF blends were made to form a strong hydrophilic membrane. ZrO_2 nano-sized particle (45 nm) is used as an inorganic material because of its ability to reduce fouling and increase the hydrophilicity of membrane. PVP was used as a pore former and DMAC as a solvent. The performances of prepared membranes were investigated. To evaluate the surface hydrophilicity, contact angles of the membranes were measured. The characterization of the membranes was carried out using scanning electron microscopy (SEM), Fourier transform infrared (FTIR) and X-ray diffraction (XRD). The petroleum refinery effluent was used as a feed in the UF process and also similar oily water were prepared in laboratory for large-scale experimentation.

2. Experimental details

2.1. Materials

Polyvinylidene fluoride with 98% purity procured from Sigma-–Aldrich, US was used as a membrane polymer. Polyethersulphone (PES crystal 5200 with M_w = 49,000 g/mol) provided by Solvay India limited, dimethylacetamide (DMAC), polyvinylpyrrolidone (PVP, with M_w = 40,000 g/mol), sodium hexametaphosphate and zirconia nanoparticle of size 45 nm was procured from Sisco Research Laboratory (SRL), India. Isopropyl alcohol and distilled water procured from Gyan Scientific, India were used as non-solvents. The refinery effluent used was collected from Indian Oil Corporation Limited Refinery, Panipat India.

2.2. Method

2.2.1. Sulphonation of PES

Sulphonation of PES was carried out using a glass reactor equipped with a magnetic stirrer. Sulphuric acid was used as the sulphonation agent as well as solvent for sulphonation of PES. The polymer dissolution time was 3 h and temperature was kept at 20˚C. Sulphonated polyethersulphone was precipitated using ice cold water under stirring. The precipitate was recovered by filtration and washed repeatedly with distilled water. Finally, the SPES was dried under vacuum at 50˚C for 24 h [29].

2.2.2. Preparation of PVDF membranes blended with SPES and ZrO_2 nanoparticles

The flat sheets of membranes were prepared by phase inversion method. The blend of two polymers (PVDF and SPES) was prepared using DMAC as the common solvent. The ratio of PVDF to SPES was kept as 60:40 in all samples. The ZrO_2 particles were dispersed in a sodium thiosulphate solution and the mixture was sonicated for 2 h. It was then added into the casting solution of polymers. Small amount of PVP (4 wt% of solution) was added in to the casting solution as a pore-forming agent.

For homogeneous mixing of solution, the stirring was done at 600 rpm for 24 h at 35˚C. After stirring, the homogeneous polymer composite solution was kept at 35˚C for 24 h to remove air bubbles. The membrane (with 200 μm thickness) was casted on a glass plate using a membrane casting applicator. The casted membrane was immediately transferred to distilled water for 1 h. The membrane was then kept in isopropyl alcohol for additional 1 h to remove the water completely. The membrane was then sandwiched between the two

sheets of filter paper and dried for 24 h in an air oven at 50˚C. Using this procedure, 10 membranes having 4 wt% nanoparticles of ZrO_2, 1 membrane with 2 wt% ZrO_2 particles and another membrane without ZrO_2 particles were prepared. It was observed that addition of more than 4 wt% ZrO_2 particles in the casting solution results in the deformation of membrane structure and decrease in its tensile strength. The compositions of casting solutions used are reported in Table 1.

2.3. Characterization of membranes

2.3.1. Measurement of contact angle and evaluation of mechanical properties

Membrane–water contact angle was measured using Kruss F-100 tensiometer, Germany to investigate the changes in the surface wetting characteristics of PVDF–SPES–ZrO_2 composite UF membrane. Deionized water was used as the test liquid in all the measurements. The water droplets were spread on the surface of the membrane and the contact angle of the droplet with the surface was measured using the contact angle measuring instrument. The tensile strength and elongation at break of the membranes were obtained using Instron 3369 tensile testing machine at the School of Material Science and Technology (SMST), IIT (BHU).

2.3.2. XRD, FTIR and SEM analyses

The XRD analysis was carried out using an X-ray diffractometer, RIGAKU Bruker AXS D8 Germany. The diffraction analysis was carried out from $10^\circ \le 2\theta \le 70^\circ$ at a scan speed of 2°/min to obtain the crystal structure and the phases present in the samples. FTIR analysis was performed to obtained spectroscopic data of PVDF–SPES–ZrO_2 composite membrane using a Thermo Nicolet 5700, USA. The FTIR spectra were recorded for 36 scans with 4-cm^{-1} resolution between 500 and 4,500 cm^{-1}.

The surface and cross-sectional morphology was characterized by SEM (EVO MA 15 ZEISS) Germany. The membranes were cut into small sizes and cleaned with filter paper. These pieces were immersed in liquid nitrogen for 15 s and frozen. Frozen samples of the membrane were broken and dried in air. All the samples were gold coated by sputtering before taking SEM images.

2.3.3. Effect of ZrO_2 nanoparticles on water content

Water retention capacity of the membrane was calculated from the experimentally determined weight of dry and wet membrane pieces as follows:

$$W_c = \frac{W_{wet} - W_{dry}}{W_{wet}} \times 100 \quad (1)$$

where W_c is the water content of the membranes, and W_c and W_{dry} are the wet and dry weights of the membranes, respectively.

2.4. Quality of petroleum refinery effluent

The petroleum refinery effluent was obtained from the Indian Oil Corporation Limited refinery located at Panipat, India. The total dissolved solids (TDS), turbidity, total suspended solids (TSS), biological oxygen demand (BOD), chemical oxygen demand (COD), total organic carbon (TOC) and oil and grease contents were determined before and after ultrafiltration runs using standard methods [30]. The turbidity was analysed using a turbidity meter, LAB-VIS Aqualytic, Germany and the COD and TOC were determined using Shimadzu UV spectrophotometer, Japan and Shimadzu 5000 TOC analyzer, Japan, respectively.

2.5. Fouling experiments

The filtration experiments were carried out using tangential low filtration (ultrafiltration unit), Tandem Germany at a temperature of 35˚C. The experiments were performed for 90 min with a prepared membrane. After 90 min, the used membrane was replaced with fresh membrane and the velocity was increased. The composition of all the membranes used in the

Table 1
Composition of casting solution

PVDF + SPES (wt%)	PVP (wt%)	ZrO_2 (wt%)	DMAC (wt%)	Name of membranes
20.0	4.0	0.0	76	P1
18.0	4.0	2.0	76	P2
16.0	4.0	4.0	76	P3

experiments was same except for last experiment where the composition of nanoparticles was varied. The transmembrane pressure was varied from 0.1 to 0.5 MPa and feed velocity from 1 to 5 m/s. Fouling is the resistance during filtration and cleaning is required for reducing this resistance. The main cause of fouling is the formation of cake and/or gel layer on the membrane surface. The flux (J) value through the cake and the membrane may be described by the following equation [31]:

$$J = \frac{m}{(A\Delta t)} \tag{2}$$

where m is the mass of permeated water, A is the membrane cross-sectional area and Δt is the permeation time.

The UF membrane was evaluated for treatment of refinery effluent with a fixed loss of the initial flux, using cross-flow of permeate with respect to retentate. The flow meter was connected to measure the feed rate, permeate flux, retentate as well as to test the fouling. Distilled water was fed from the permeate side, in the reverse direction for backwashing. The fouling time calculation for loss of initial flux up to a certain percentage of their initial flux helps in evaluating the membranes antifouling property [32].

3. Results and discussion

3.1. Physical properties of membranes

A contact angle was found to be 81.4° for pure polymer membrane, 73.4° for 2% ZrO_2 nanoparticle-added membrane and 57.3° for 4% ZrO_2 nanoparticle-added membrane. The corresponding bulk porosity was 62.1, 73.6 and 81.4%, respectively. Decreasing the contact angle with the addition of ZrO_2 nanoparticles indicates that the membrane is becoming more and more hydrophilic. The increase in porosity with the addition of ZrO_2 nanoparticles indicates higher permeate flux.

The tensile strength was 12.1, 16.5 and 19.2 MPa for pure polymer membrane, 2% ZrO_2 nanoparticle-added membrane and 4% ZrO_2 nanoparticle-added membrane, respectively. Whereas the elongation at break point was 3.93, 4.63 and 5.92%, respectively, for pure polymer membrane, 2% ZrO_2 nanoparticle-added membrane and 4% ZrO_2 nanoparticle-added membrane. These values indicate that the membrane matrix is becoming more resistant to deformation with the addition of ZrO_2 nanoparticles.

3.2. XRD and FTIR analyses of entrapped PVDF–SPES–ZrO_2 membrane

The peak positions for PVDF–SPES hydrophilic membrane (Fig. 1) appear at 2θ values of nearly 19°, 20°, 27°, 35°, 39° and 43° and relative intensities obtained for the polymer matches with the JCPDS Card no. 38-1638 file. The occurrence of ZrO_2 crystalline phase is disrupted according to the results obtained from the XRD analysis (Figs. 2 and 3). This indicates that the crystalline behaviour of amorphous PVDF–SPES membrane is affected by the presence of ZrO_2 nano-sized particles in the casting solution. The peaks for PVDF–SPES/4 wt% ZrO_2 hydrophilic membrane appear at 2θ values of 18°, 25°, 28°, 35°, 50° and 57° (Fig. 1) and the peaks for PVDF–SPES/2 wt% ZrO_2 hydrophilic membrane appear at 2θ values of 18°, 20°, 28°, 36° and 48° (Fig. 3). Variation in peaks indicates the effect of interaction between the polymer and ZrO_2 nanoparticles. This may be due to the decrease in polymer concentration caused by ZrO_2 nanoparticles entrapment. The peaks of PVDF–SPES/4 wt% ZrO_2 and PVDF–SPES/2 wt% ZrO_2 hydrophilic membranes also indicate the peaks of ZrO_2 crystal through File No. 37-1484. Similar peaks of PVDF is reported by Shao et al. [27], Campos et al. [33] and Devikala et al. [34], and that of ZrO_2 crystal is reported by Matos et al. [35] and Ananta et al. [36].

The FTIR spectra of PVDF–SPES with 4 wt% ZrO_2-, without ZrO_2- and 2 wt% ZrO_2-entrapped membranes are shown in Figs. 4–6. The area of the OH stretching in the spectrum of ZrO_2-entrapped PVDF–SPES membrane (due to absorbed water molecules) was found to exhibit strong band of asymmetric vibration at 3,040 and 2,112 cm^{-1} (Fig. 4). The sharp and weak peaks

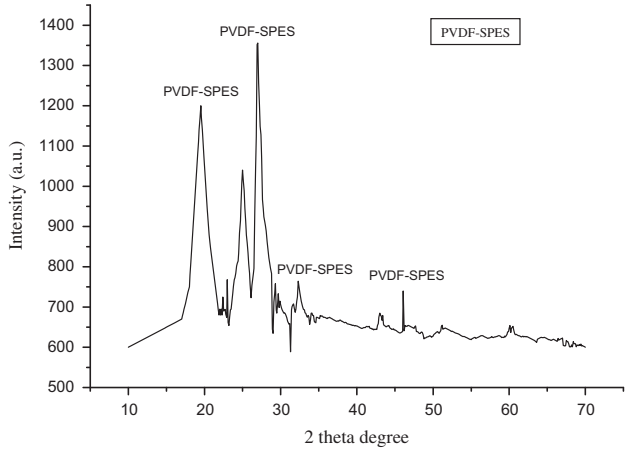

Fig. 1. XRD of SPES–PVDF polymeric membrane with 0 wt% ZrO_2 nanoparticles.

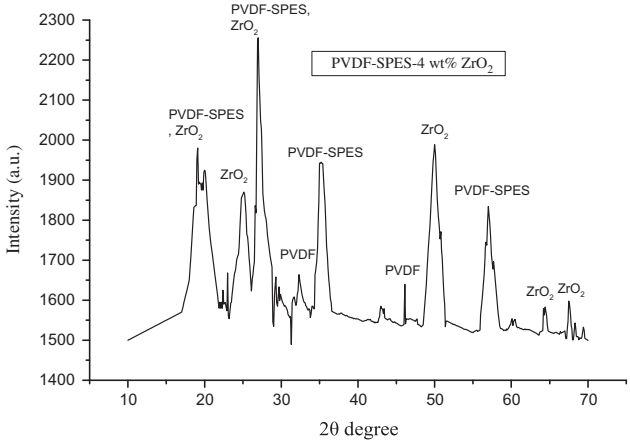

Fig. 2. XRD of SPES–PVDF polymeric membrane modified with 4 wt% ZrO_2 nanoparticles.

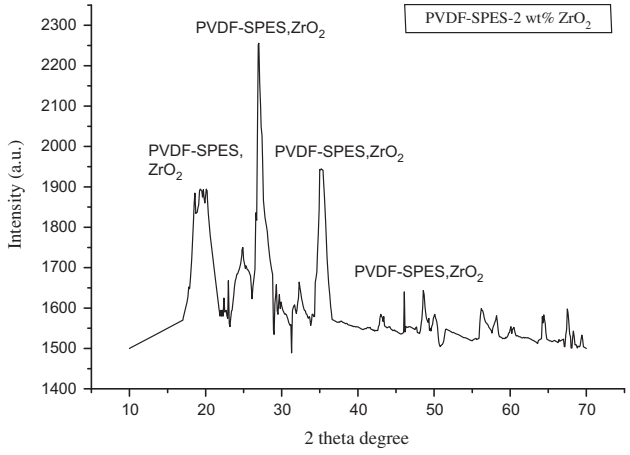

Fig. 3. XRD of SPES–PVDF polymeric membrane modified with 2 wt% ZrO_2 nanoparticles.

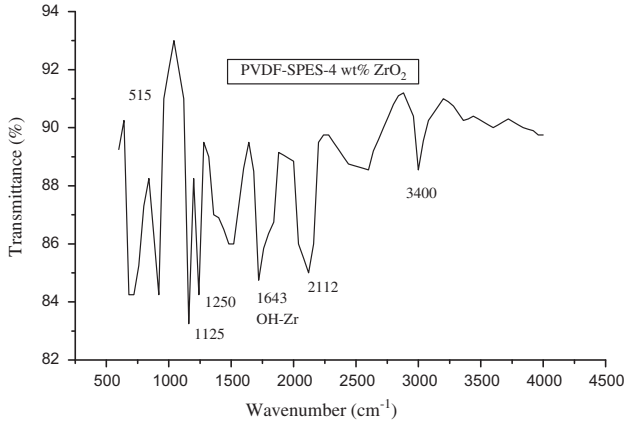

Fig. 4. FTIR of SPES–PVDF polymeric membrane modified with 4 wt% ZrO_2 nanoparticles.

were found at 1,250 and 515 cm^{-1}, suggesting the presence of tetragonal and monoclinic ZrO_2, respectively. The high intensities of these bands can be explained by the high affinity of ZrO_2 nanoparticle entrapment in the structure of PVDF–SPES membrane. There exists an adsorption of non-bridging OH-groups at 1,673 cm^{-1} (Fig. 4). The peaks of PVDF–SPES membrane appear at 775 and 700 cm^{-1} (Fig. 5). The peaks of PVDF–SPES/2 wt% ZrO_2 membrane appear at 750, 1,340, 1,640 and 2,620 cm^{-1} (Fig. 6). Khayet and Payo have also reported the spectra of neat PVDF–SPES membrane at 3,200–3,400 cm^{-1} [37].

3.3. Membrane morphology

Fig. 7(a) and (b) is the cross-sectional images of PVDF–SPES/4 wt% ZrO2 membrane at 1.5K× magnification and at 700×, respectively. Fig. 7(c) and (d) is the surface images of PVDF–SPES/4 wt% ZrO_2 at 983× and 15K× magnifications, respectively. The cross-sectional and surface SEM images of all samples are clearly indicating the membrane structure. The cross-sectional morphology of the membrane having 4% ZrO_2 nanoparticles shows that ZrO_2 particles are uniformly distributed on the membrane surface (Fig. 7(a) and (b)). Fig. 8(a) is the cross-sectional image of 0 wt% ZrO_2 at 1.50K×, Fig. 8(b) is the surface image of 0 wt% ZrO_2 at 700× and Fig. 8(c) is the cross-sectional image of 2 wt% ZrO_2 at 983×.

The SEM photomicrographs of cross-section and surface of the membrane indicated the formation of large macro voids in the sublayer (Fig. 8). The surfaces of the membranes are composed of micro-porous structures with a large number of pores. Both

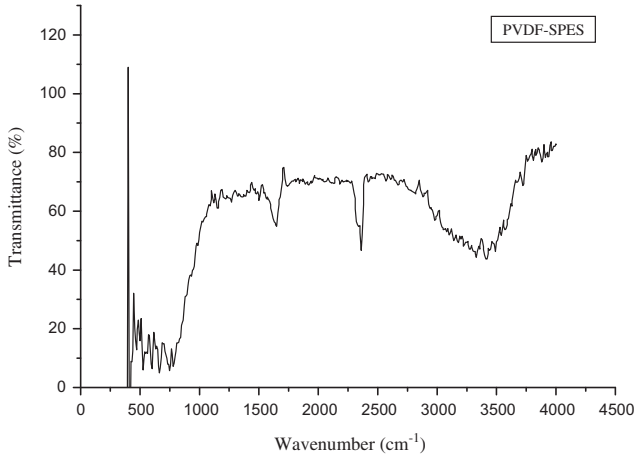

Fig. 5. FTIR of SPES–PVDF polymeric membrane modified with 0 wt% ZrO_2 nanoparticles.

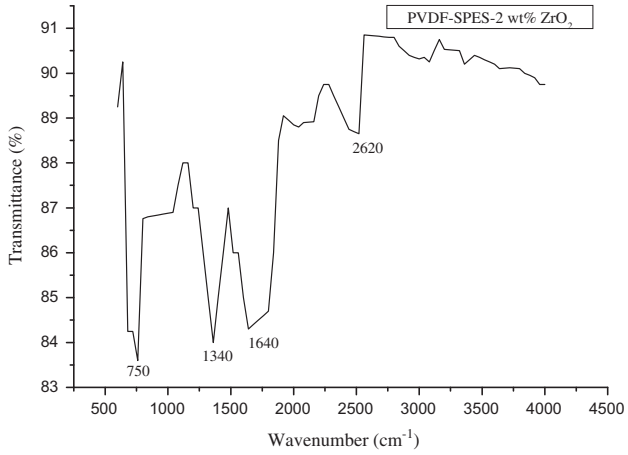

Fig. 6. FTIR of SPES–PVDF polymeric membrane modified with 2 wt% ZrO_2 nanoparticles.

interconnected holes and their networks are composed of micro-spherical particles connected with each other. The ZrO_2 nanoparticles are also present inside and outside the pores forming a nanolevel roughness (Figs. 7 and 8).

3.4. Evaluation hydrophilicity, performance and antifouling properties

The hydrophilicities of modified and un-modified membranes differ as shown in Fig. 9. The contact angles of the membranes decrease as the concentration of ZrO_2 nanoparticles increases from 0 to 4%. The higher affinity of ZrO_2 nanoparticles to water results in a decrease in the value of contact angle suggesting an increase in the hydrophilicity.

Fig. 9 shows the plots of water flux vs. transmembrane pressure for all the membranes with and without zirconia. It is seen that maximum flux is obtained with 4% zirconia-loaded membrane. The increase in water flux with increasing ZrO_2 concentration is due to increase in the porosity of the membrane from 0.621 for pure polymeric membrane to 0.814 for membrane with 4 wt% ZrO_2. It is further seen that for all

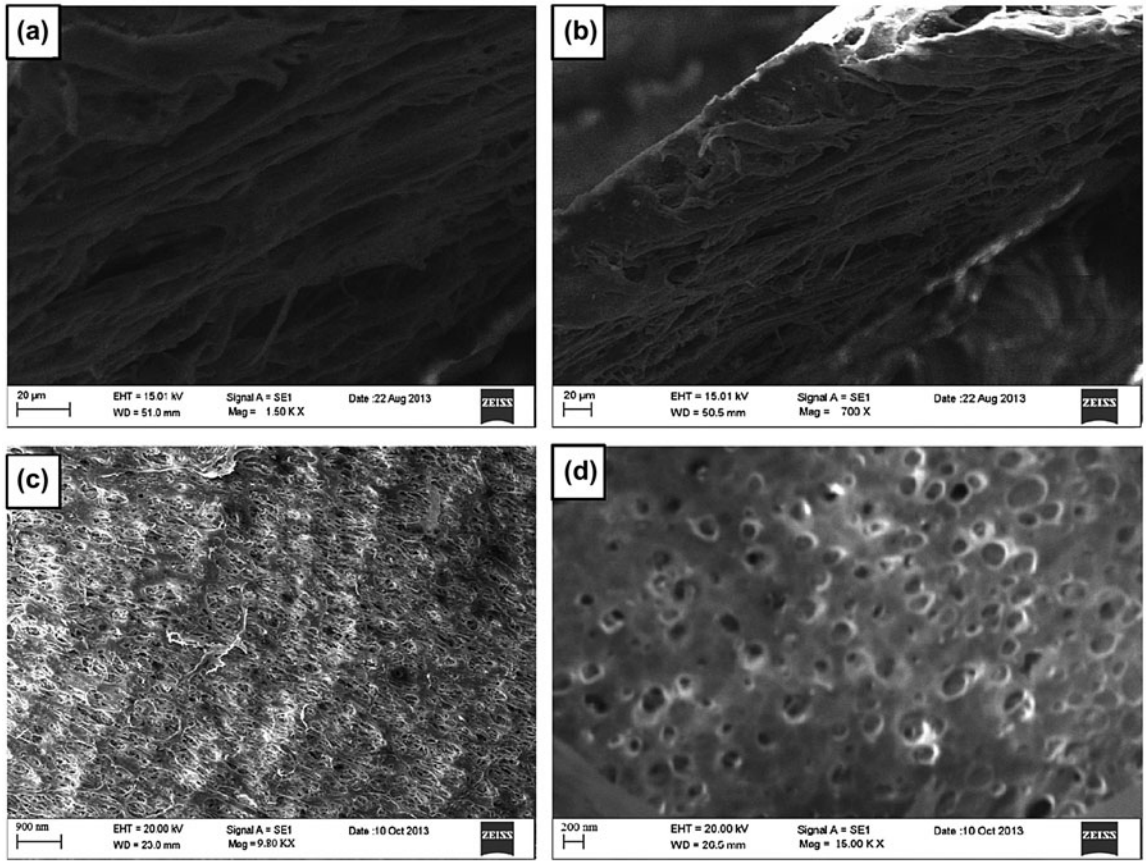

Fig. 7. Cross-sectional and surface SEM images of SPES–PVDF–ZrO_2 membranes (a) cross-sectional image of 4 wt% ZrO_2 at 1.50K×, (b) cross-sectional image of 4 wt% ZrO_2 at 700×, (c) surface image of 4 wt% ZrO_2 at 983× and (d) surface image of 4 wt% ZrO_2 at 15.00K×.

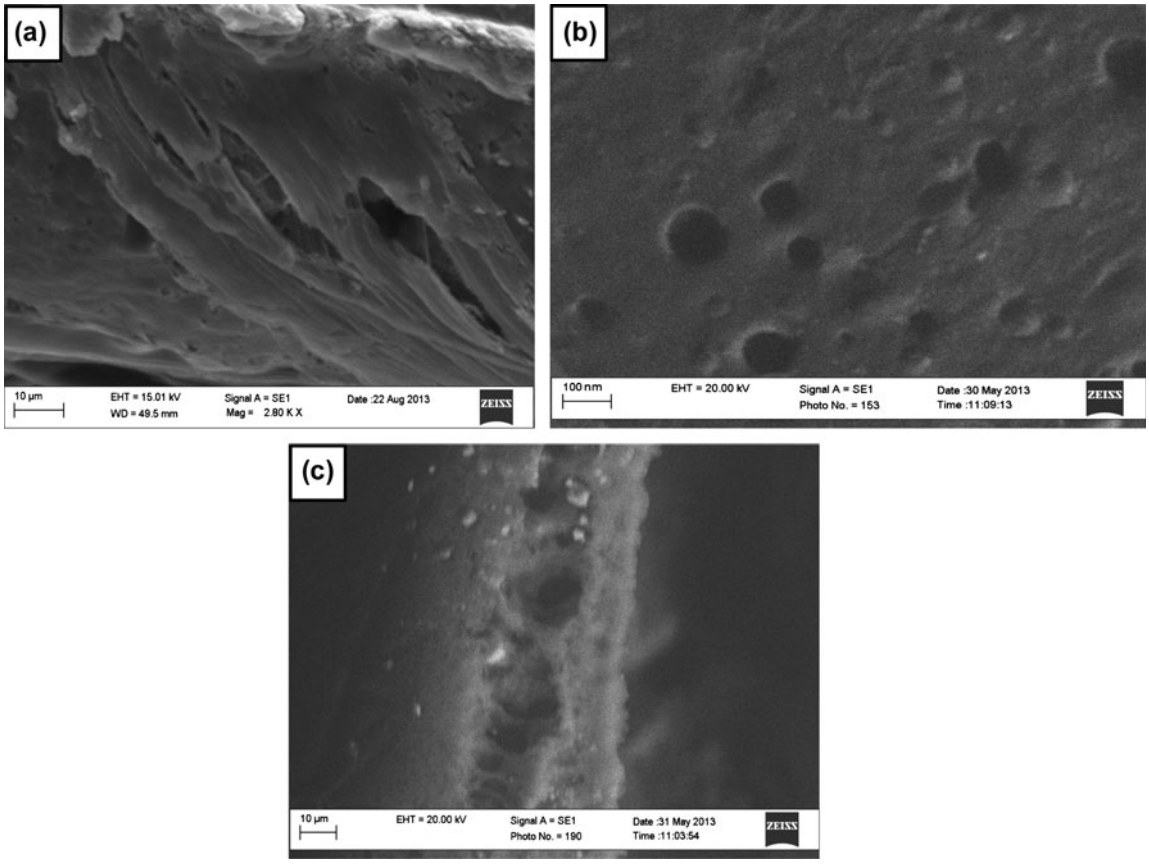

Fig. 8. Cross-sectional and surface SEM images of SPES–PVDF–ZrO_2 membranes (a) cross-sectional image of 0 wt% ZrO_2 at 1.50K×, (b) surface image of 0 wt% ZrO_2 at 700× and (c) cross-sectional image of 2 wt% ZrO_2 at 983×.

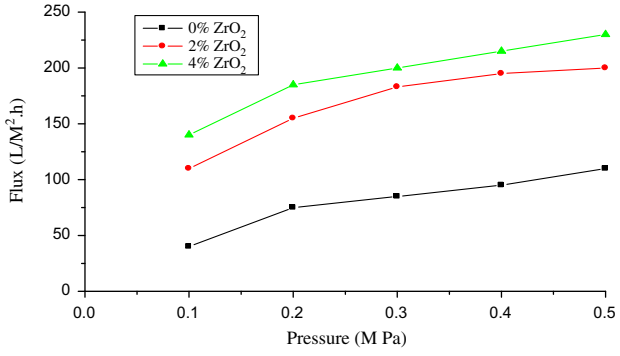

Fig. 9. Water flux vs. transmembrane pressure for UF membranes prepared using different concentration of nano-sized ZrO_2 particles.

the three membranes, water flux increases with increasing pressure up to a certain value and then tends towards a constant value at higher pressures indicating the stabilization of various resistances.

Fig. 10 shows a plot of permeate flux obtained for petroleum refinery effluent against time by varying pressure from 0.1 to 0.5 MPa and flow velocity from 1 to 5 m/s. It is seen that the flux declines up to the first 45 min, and thereafter, it becomes constant at all pressures and velocities. As the UF continues, the membrane fouling increases up to first 45 min and then becomes more or less constant resulting in a constant resistance causing ultrafiltration flux.

3.5. Influence of accelerating feed velocity

Fig. 11 shows permeate flux vs. time plot for membranes (4 wt% ZrO_2) at various feed velocities (1–5 m/s) and pressures (0.1–0.5 MPa) with intermittent backwashing for 30 s after every 30 min of use. It is seen that the backwashing is capable of restoring the flux to about 90% of its initial value. However, slight decline is observed after each successive washing, which can be attributed to membrane compaction and interaction between membrane polymers, and contaminants present in the feed wastewater.

Table 2
Petroleum refinery effluent and UF permeate characteristics

Parameters	Turbidity (NTU)	COD (mg l^{-1})	BOD (mg l^{-1})	TOC (mg l^{-1})	Oil and grease (mg l^{-1})	TDS (mg l^{-1})	TSS (mg l^{-1})
Raw feed[a]	55	160	54	84	76	2,250	32
UF permeate	1.21	42	19	18.5	0.23	1,450	0.7
% Removal	97.8	73.75	64.8	78	99.7	35.6	97.8
CPCB standards for reuse[b]	–	125	15	–	5	–	20

[a]Present work.
[b]Ref. [38].

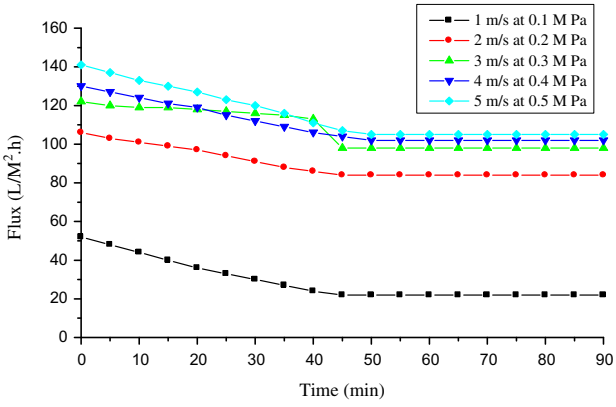

Fig. 10. Permeate flux vs. time plots for SPES–PVDF polymeric membrane modified with 4 wt% ZrO_2 nanoparticles without backwashing: effect of transmembrane pressure and velocity.

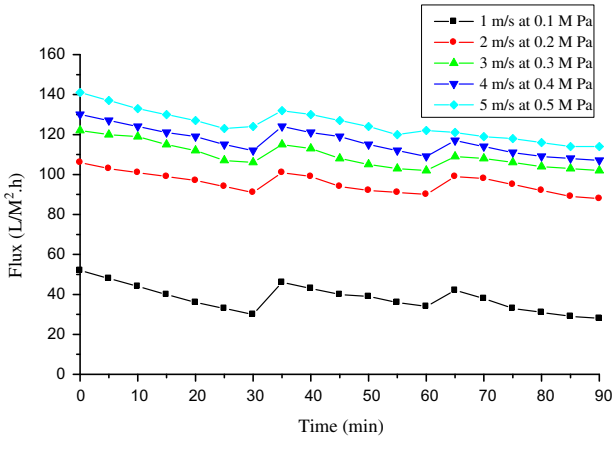

Fig. 11. Permeate flux vs. time plots for SPES–PVDF polymeric membrane modified with 4 wt% ZrO_2 nanoparticles with backwashing for 30 s after every 30 min: effect of transmembrane pressure and velocity.

3.6. Evaluation of removal efficiency

In order to assess the effectiveness of ZrO_2-added membrane in removing turbidity, oil and grease, TDS, TSS, COD, BOD and TOC, ultrafiltration tests were performed with refinery effluent using (4 wt% ZrO_2) membrane. The values of various parameters of refinery effluent before and after ultrafiltration are reported in Table 2. It can be seen that the membrane is capable of removing about 98% of oil and grease, turbidity and TSS. The COD and TOC reduction is around 73.8 and 78%, respectively, the BOD reduction is only around 65% only.

3.7. Evaluation of fouling recovery ratio

The initial and final fluxes of the membranes containing 4 wt% ZrO_2 are shown in Figs. 10 and 11. The fouling recovery ratio for continuous UF process shown in Fig. 10 are 136, 26, 24, 27 and 34% at TMP of 0.1, 0.2, 0.3, 0.4 and 0.5 MPa, respectively, and the fouling recovery ratio for UF process as shown in Fig. 6 (backwash after 30 min) are 85, 20, 19, 21 and 23% at TMP of 0.1, 0.2, 0.3, 0.4 and 0.5 MPa, respectively. The best value of permeate flux with low fouling recovery ratio was obtained at the feed velocity of 3 m/s and transmembrane pressure of 0.3 MPa (3 bars).

4. Conclusions

Highly hydrophilic PVDF–SPES membranes with good antifouling property are prepared by addition of ZrO_2 nanoparticles in the casting solution. The membranes were fabricated using the phase inversion method. The XRD, FTIR and SEM studies confirm the presence of ZrO_2 nanoparticles on the surface of the membrane. The values of contact angle indicated an increase in surface hydrophilicity of the ZrO_2-modified membrane. Tensile strength and elongation at the

break point values of modified membranes are increased by more than 60%. The long-term flux stability and antifouling properties of 4 wt% ZrO_2-modified membrane are improved. The prepared UF membranes 4 wt% ZrO_2 can efficiently remove suspended solids (97.8%), turbidity and oil content (99.7%) and organic compounds (78%).

The application of modified hydrophilic membrane having high antifouling properties causes reduction in the permeate flux. The operating conditions have little effect on permeate quality.

Acknowledgement

The authors gratefully acknowledge the laboratory facility provided by Co-ordinator TBI, Department of Chemical Engineering and Technology, IIT (BHU), Varanasi, India.

References

[1] P. Agarwal, P.K. Mishra, P. Srivastava, Statistical optimization of the electrospinning process for chitosan/polylactide nanofabrication using response surface methodology, J. Mater. Sci. 47(10) (2012) 4262–4269.
[2] L. Yan, Y. Shui, C.B. Xiang, S. Xianda, Effect of nano-sized Al_2O_3-particle addition on PVDF ultrafiltration membrane performances, J. Membr. Sci. 276 (2005) 162–167.
[3] B. Tansel, J. Regula, R. Shalewitz, Treatment of fuel oil and crude oil contaminated waters by ultrafiltration membranes, Desalination 102 (1995) 301–311.
[4] S. Weigert, M. Sára, Surface modification of an ultrafiltration membrane with crystalline structure and studies on interactions with selected protein molecules, J. Membr. Sci. 106 (1995) 147–159.
[5] B. Jung, Preparation of hydrophilic polyacrylonitrile blend membranes for ultrafiltration, J. Membr. Sci. 229 (2004) 129–136.
[6] J. Marchese, M. Ponce, N.A. Ochoa, P. Prádanos, L. Palacio, A. Hernández, Fouling behaviour of polyethersulfone UF membranes made with different PVP, J. Membr. Sci. 211 (2003) 1–11.
[7] R. Abedini, S.M. Mousavi, R. Aminzadeh, A novel cellulose acetate (CA) membrane using TiO_2 nanoparticles: Preparation, characterization and permeation study, Desalination 277 (2011) 40–45.
[8] L. Yan, Y.S. Li, C.B. Xiang, Preparation of poly(vinylidene fluoride)(pvdf) ultrafiltration membrane modified by nano-sized alumina (Al_2O_3) and its antifouling research, Polymer 46 (2005) 7701–7706.
[9] J. Ahn, W.J. Chung, I. Pinnau, M.D. Guiver, Polysulfone/silica nanoparticle mixed matrix membranes for gas separation, J. Membr. Sci. 314 (2008) 123–133.
[10] L.Y. Yu, Z.L. Xu, H.M. Shen, H. Yang, Preparation and characterization of PVDF-SiO_2 composite hollow fiber UF membrane by sol–gel method, J. Membr. Sci. 337 (2009) 257–265.
[11] J. Xu, Z.L. Xu, Poly(vinyl chloride) (PVC) hollow fiber ultrafiltration membranes prepared from PVC/additives/solvent, J. Membr. Sci. 208 (2002) 203–212.
[12] T.S. Chung, Z.L. Xu, W.H. Lin, Fundamental understanding of the effect of air-gap distance on the fabrication of hollow fiber membranes, J. Appl. Polym. Sci. 72 (1999) 379–395.
[13] T.N. Shah, H.C. Foley, A.L. Zydney, Development and characterization of nanoporous carbon membranes for protein ultrafiltration, J. Membr. Sci. 295 (2007) 40–49.
[14] A. Bottino, G. Capannelli, A. Comite, Preparation and characterization of novel porous PVDF-ZrO_2 composite membranes, Desalination 146 (2002) 35–40.
[15] C. Teodosiu, O. Pastravanu, M. Macoveanu, Neural network models for ultrafiltration and backwashing, Wat. Res. 34 (2000) 1371–1380.
[16] M.L. Luo, J.Q. Zhao, W. Tang, C.S. Pu, Hydrophilic modification of poly(ether sulfone) ultrafiltration membrane surface by self-assembly of TiO_2 nanoparticles, Appl. Surf. Sci. 249 (2005) 76–84.
[17] C.C. Teodosiu, M.D. Kennedy, H.A.V. Straten, J.C. Schippers, Evaluation of secondary refinery effluent treatment using ultrafiltration membranes, Wat. Res. 33 (1999) 2172–2180.
[18] A.K. Plappally, J.H. Lienhard V, Energy requirements for water production, treatment, end use, reclamation, and disposal, Renew. Sust. Energy Rev. 16 (2012) 4818–4848.
[19] E. Zondervan, B.H.L. Betlem, B. Roffel, Development of a dynamic model for cleaning ultra filtration membranes fouled by surface water, J. Membr. Sci. 289 (2007) 26–31.
[20] M. Cheryan, N. Rajagopalan, Membrane processing of oily streams: Wastewater treatment and waste reduction, J. Membr. Sci. 151 (1998) 13–28.
[21] S.R.P. Shariati, B. Bonakdarpour, N. Zare, F.Z. Ashtiani, The effect of hydraulic retention time on the performance and fouling characteristics of membrane sequencing batch reactors used for the treatment of synthetic petroleum refinery wastewater, Bioresour. Technol. 102 (2011) 7692–7699.
[22] S. Mishra, S. Sachan, P.K. Mishra, Preparation and application of SPPEES-TiO_2 composite micro-porous UF membrane for refinery effluent treatment, Int. J. Environ. Res. Dev. 4(2) (2014) 147–152.
[23] S.B. Mishra, S. Sachan, P.K. Mishra, Preparation and characterisation of PPEES-TiO_2 composite microporous UF membrane for oily water treatment, Proc. Mater. Sci. 5 (2014) 123–129.
[24] M. Ebrahimi, D. Willershausen, K.S. Ashaghi, L. Engel, L. Placido, P. Mund, P. Bolduan, P. Czermak, Investigations on the use of different ceramic membranes for efficient oil-field produced water treatment, Desalination 250 (2010) 991–996.
[25] C. Mu, Y. Su, M. Sun, W. Chen, Z. Jiang, Remarkable improvement of the performance of poly(vinylidene fluoride) microfiltration membranes by the additive of cellulose acetate, J. Membr. Sci. 350 (2010) 293–300.
[26] J.M. María Arsuaga, A. Sotto, G.D. del Rosario, A. Martínez, S. Molina, S.B. Teli, J.D. de Abajo, Influence of the type, size, and distribution of metal oxide particles on the properties of nanocomposite ultrafiltration membranes, J. Membr. Sci. 428 (2013) 131–141.

[27] L. Shao, Z.X. Wang, Y.L. Zhang, Z.X. Jiang, Y.Y. Liu, A facile strategy to enhance PVDF ultrafiltration membrane performance via self polymerized polydopamine followed by hydrolysis of ammonium fluotitanate, J. Membr. Sci. 461 (2014) 10–21.
[28] Z.X. Wang, C.H. Lau, N.Q. Zhang, Y.P. Bai, L. Shao, Mussel-inspired tailoring of membrane wettability for harsh water treatment, J. Mater. Chem. A 3 (2015) 2650–2657.
[29] A. Salahi, M. Abbasi, T. Mohammadi, Permeate flux decline during UF of oily wastewater: Experimental and modeling, Desalination 251 (2010) 153–160.
[30] Central Pollution Control Booard (CPCB), India, Guide manual: Water and waste water analysis.
[31] A. Rahimpour, M. Jahanshahi, B. Rajaeian, M. Rahimnejad, TiO_2 entrapped nano-composite PVDF/SPES membranes: Preparation, characterization, antifouling and antibacterial properties, Desalination 278 (2011) 343–353.
[32] N. Maximous, G. Nakhla, W. Wan, K. Wong, Performance of a novel ZrO_2/PES membrane for wastewater filtration, J. Membr. Sci. 352 (2010) 222–230.
[33] J.S.C. de C. Campos, A.A. Ribeiro, C.X. Cardoso, Preparation and characterization of PVDF/$CaCO_3$ composites, Mater. Sci. Eng. B 136 (2007) 123–128.
[34] S. Devikala, P. Kamaraj, M. Arthanareeswari, Fabrication of PVDF composites and their electrical conductivity studies, IJIRS 2(11) (2013) 359–367.
[35] J.M.E. Matos, F.M. Anjos Júnior, L.S. Cavalcante, V. Santos, S.H. Leal, L.S. Santos Júnior, M.R.M.C. Santos, E. Longo, Reflux synthesis and hydrothermal processing of ZrO_2 nanopowders at low temperature, Mater. Chem. Phys. 117 (2009) 455–459.
[36] S. Ananta, R. Tipakontitikul, T. Tunkasiri, Synthesis, formation and characterization of zirconium titanate (ZT) powders, Mater. Lett. 57 (2003) 2637–2642.
[37] M. Khayet, M.C.G. García-Payo, X-ray diffraction study of polyethersulfone polymer flat sheet and hollow fibers prepared from the same under different gas-gaps, Desalination 245 (2009) 494–500.
[38] Central Pollution Control Board, India, The environmental protection rules 1986, gazette no. 66 (1987) 6–2.